

Negative Magnetoresistivity in Tl_4Se_3S Crystals

Atef Fayez Qasrawi

Department of Physics, Arab American University, Jenin, Palestine

atef.qasrawi@aauj.edu

Abstract

The temperature and magnetic field dependencies of the magnetoresistivity of Tl_4Se_3S crystals have been measured in the temperature region of 195-310 K at magnetic fields up to 1.4 T. The magnetoresistivity is observed to exhibit negative values at all measured temperatures. Increasing the magnetic field intensity leads to larger values of negative magnetoresistivity. The magnetoresistivity as a function of applied field was described by the Khosla-Fischer model for spin scattering of carriers in an impurity band. The temperature dependence of magnetoresistivity has revealed the existence of paramagnetic-ferromagnetic and ferromagnetic-paramagnetic phase transitions at 270 and 220 K, respectively. The existence of these transitions is attributed to the domination of localized spin scattering (magnetic scattering) in the temperature region of 220-270 K and the domination of thermal lattice scattering in the remaining temperature regions.

PACS: 72.10.Di , 72.15.Rn , 73.50.Bk, 71.55.Ht

Keywords : Resistivity, Chain crystals, Tl_4Se_3S , Magnetization.

Introduction

Magnetoresistive sensors used for data storing play a vital role in information technology. Currently, the giant magnetoresistivity is used in most of the hard drive reading heads. The reading head itself, which travels above a storage disk, is composed of magnetoresistive material connected to a current source. Today, the fundamental physical limits of the available technology have been reached. For this reason, within the last decade a new approach using the spin of electrons instead of the charges has been developed (Kent, and Worledge, 2015). Devices, which get use of magnetoresistive effect, have become more attractive. For example, some devices are built upon the giant magnetoresistivity (Kokkinis et al., 2015; Nicolás et al., 2015) and tunnel magnetoresistivity effects (Bin et al., 2015).

Previously, we investigated the temperature and photo-excitation effects on the electrical properties of the Tl_4Se_3S crystals (Qasrawi and Gasanly, 2010). The study helped determine the impurity and recombination states in the crystals. In addition, a linear photo-response of photocurrent as a function of the illumination intensity at room temperature has been observed; the latter gives an indication about the usability of the crystal in photo-detection. For the purpose of finding a new technological application, the present article describes and analyzes the magnetoresistivity behavior of the semiconducting (Tl_4Se_3S) bulk compound. This crystal belongs to the $TlMX_2$ ($M = Ga, In; X = Se, S, Te$) group of semiconductors (Shim et al., 2015; Zalamai et al., 2015; Yildirim et al., 2015; Isik et al., 2015; Guler, 2014; Qasrawi, and Gasanly, 2006). Such compounds are known as low-dimensional materials that have high anisotropic properties. The atomic arrangement of this type of crystals forces the conduction carriers to move in only one or two directions. This type of forced motion, which reveals abnormal physical properties, seems to be a good candidate for future technological applications. Tl_2S and Tl_2Se nanorods have been synthesized via solvothermal route with the addition of KI (Youbao et al., 2004). Furthermore, an accumulating cell made on the basis of a p-TlSe single crystal and aqueous LiCl solution was also fabricated. The maximum *emf.* of the cell was reported as 2.1 V, the short-circuit current density reached 100 mA/cm^2 for a fully charged cell, and the discharging depth amounted to 95% (Guseinov et al., 1986).

Experimental Details

Single crystals of Tl_4Se_3S crystals were grown by the Bridgman method from the stoichiometric melt of the starting materials sealed in evacuated (10^{-5} Torr) silica tubes with a tip at the bottom. The ampoule was moved in a vertical furnace through a thermal gradient of

20°C/cm, between the temperatures 375 and 150°C at a rate of 6 mm/h. The analysis of X-ray diffraction data showed that $\text{Tl}_4\text{Se}_3\text{S}$ crystallized in a tetragonal unit cell, with lattice parameters: $a = 0.7975$ and $c = 0.6926$ nm. The typical dimensions of the crystals suitable for electrical measurements were $\sim 0.5 \times 0.5 \times 0.2$ cm³. Using silver paste, point contacts were fixed at the top surface of the sample. The ohmic nature of the contacts was confirmed by the I - V characteristics. These characteristics, recorded parallel to the crystal c -axis (along the chain), were found to be linear for low applied voltages.

The electrical resistivity data was recorded along the crystal c -axis in a Lake Shore 7507 Hall-effect measurements system at different temperatures and varying magnetic fields. The data was collected using an IEEE computer interface and IDEAS software provided by Lake Shore. Cooling of the sample was achieved using a closed cycle cryostat (Advanced Research Systems) and Lake Shore 340 tempera.

Results And Discussion

The magnetoresistance, which is defined as the property of a material that results in a change of resistance when exposed to a magnetic field, is rarely observed in chain crystals. Figure 1 displays the value of the electrical resistivity, $\rho(H)$, as a function of magnetic field intensity, H , for $\text{Tl}_4\text{Se}_3\text{S}$ crystals being recorded at 290 K. As it is clear, the electrical resistivity of $\text{Tl}_4\text{Se}_3\text{S}$ crystals decreases with increasing magnetic field intensity. From these data, the crystal's magnetoresistivity (ρ_m) was calculated using the relation (Khosla and Fischer, 1970),

$$\rho_m = \frac{\rho(H) - \rho(0)}{\rho(0)} \times 100 \% , \quad (1)$$

where $\rho(0)$ represents the electrical resistivity in the absence of the magnetic field.

The magnetoresistivity data obtained from equation (1) are presented in Figure 2. As displayed in the figure, the magnetoresistivity exhibits negative values. Raising the magnetic field intensity produces more negative magnetoresistivity. Such behavior may be attributed to spin scattering interactions between the localized magnetic moments of the acceptors (created by atomic vacancies and /or incomplete bonding) and the holes in an impurity band (May et al., 2004).

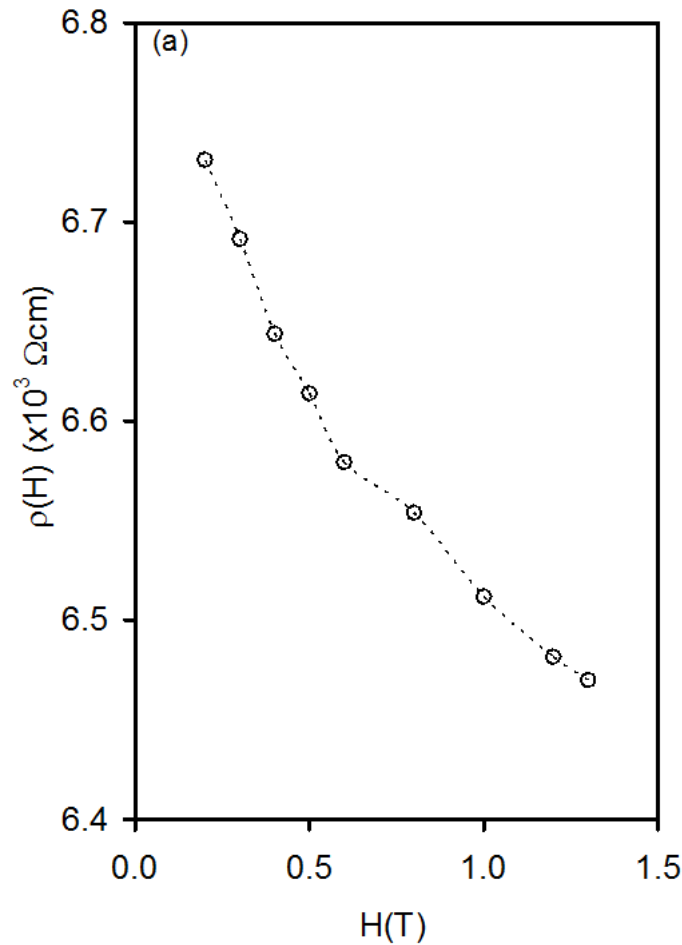


Figure 1: The $\rho(H) - H$ variation for Tl_4Se_3S crystals.

The solid line in Figure 2 represents the results of fitting the negative magnetoresistivity data using the semi-empirical equation proposed by Khosla and Fischer (Khosla and Fischer, 1970),

$$\rho_m = -B_1^2 \ln(1 + B_2^2 H^2). \tag{2}$$

The basis for this equation is Toyozawa’s localized-magnetic-moment model of magnetoresistivity, where carriers in an impurity band are scattered by the localized spin of metallic atoms (Garcia-Lekue et al., 2014) in the above equation,

$$B_1 = A_1 J \rho_F (S(S + 1) + \langle M^2 \rangle), \tag{3}$$

$$\text{and } B_2 = \sqrt{\left(1 + 4S^2 \pi^2 \left(\frac{2J\rho_F}{g}\right)^4\right)} \left(\frac{g\mu_B}{\alpha k_B T}\right). \tag{4}$$

Here, J is the exchange interaction energy, g is the Lande factor (is a geometric factor which arises in the evaluation of the magnetic interaction), ρ_F is the density of states at the Fermi energy, $\langle M \rangle$ is the average magnetization, S is the spin of the localized magnetic moment,

and α is a numerical constant ranging from 0.1 to 10. A_1 is defined as $AN_A(\sigma_j^2/\sigma_0^2)$ where A is a numerical constant, N_A is Avogadro's number, σ_j^2 is the exchange scattering cross section and σ_0^2 is due to other scattering mechanisms (such as thermal lattice scattering). Thus, A_1 can be regarded as a measure of spin based scattering. The negative magnetoresistivity data shown in Figure 2 agrees well with the Khosla-Fischer model (see the solid line in Figure 2) provided that the values of the fitting parameters B_1 and B_2 are taken as 0.35 and 8.97 (T^{-1}), respectively. These fitting parameters are consistent with literature data (May et al., 2004; Ohno et al., 1992).

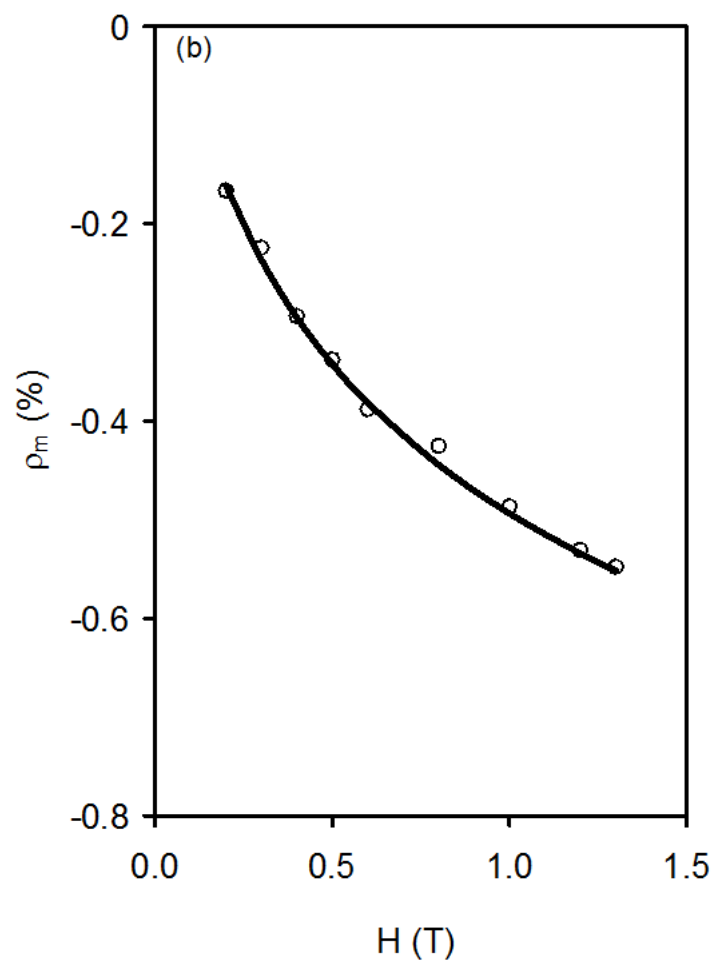


Figure 2: The magnetoresistivity–magnetic field dependence for Tl_4Se_3S crystals.

Figure 3 reflects the temperature dependence of magnetoresistivity in the temperature region of 195-310 K. The $\rho_m(T)$ dependence on T is rather different from the $\rho_0(T)-T$ dependence, which was studied and analyzed in our previous work on Tl_4Se_3S crystals (Qasrawi, and Gasanly, 2010). As it is observable from Figure 3, the magnetoresistivity increases with decreasing temperature down to a critical temperature of 270 K. Below this

temperature, the magnetoresistivity sharply decreases with temperature decreasing until it reaches 220 K, and then it starts increasing again. This behavior of magnetoresistivity in Tl_4Se_3S crystals is similar to that observed for Eu-doped perovskites $La_{0.65-x}Eu_xMnO_3$ crystals; the latter exhibited a semiconductor like and metallic like magnetoresistivity above and below critical temperatures (Curie temperature) of 352, 343, 324, 305 and 242 for x values of 0.05, 0.10, 0.15, 0.20 and 0.3, respectively (Feng et al., 2009). The metallic behavior, below T_c , was attributed to the spin based scattering (due to magnetization) which counterbalance the lattice scattering. For Tl_4Se_3S crystals, as temperature decreases below 310 K, both the intensity of thermal lattice scattering and the amount of excited charge carriers decrease. This decrement raises $\rho_m(T)$ upon temperature lowering. At temperatures near $T_c = 270$ K, the intensity of scattering, created by magnetism, become comparable to the thermal lattice scattering. As T reaches T_c , the spin transits from disorder state (paramagnetic state) to ordered state (ferromagnetic state) at temperatures just below T_c , the spin ordering ease the charge carrier transform between metal (T_I) ions and as a result $\rho_m(T)$ decreases. For this reason, at T_c , a semiconductor-metal transition is observed. Further decrease in the temperature makes the effect of the decrement of the excited charge carriers more pronounced and a metal-semiconductor transition appears again (Quan et al., 2014; Bellouz et al., 2015).

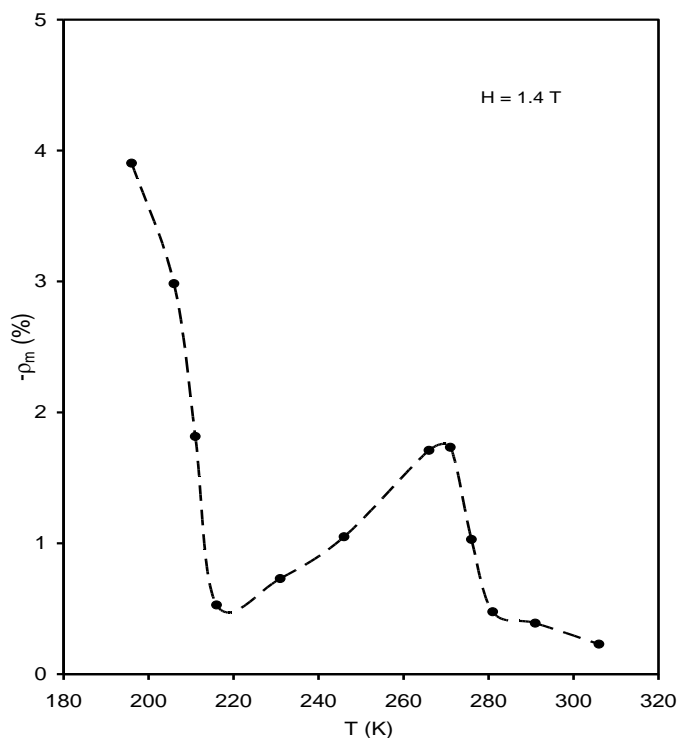


Figure 3: The temperature dependence of magnetoresistivity.

The giant magnetoresistivity along the Tl_4Se_3S crystal chains where the principle c-axis do exist is associated with a large value of Hall mobility ($873 \text{ cm}^2\text{V}^{-1}\text{s}^{-1}$) (Qasrawi, and Gasanly, 2010) along the b-axis of the crystal. The two physical parameters which appear as a response to magnetic field are worthy of consideration. The negative magnetoresistivity presented by the reduction of the electrical resistivity under the influence of magnetic field allows the manipulation of both electron spin and electron charge information technology. This indicated that the information can be stored as a particular spin orientation of itinerant electrons that carry the information a long a wire to a terminal where it can be read. The spin orientation of conduction electrons survives for relatively longtime $\sim 10^{-9}$ s compared to 10^{-14} s during which electron momentum and energy decay. This makes spintronics devices particularly attractive for memory storage and magnetic sensor applications in addition to the applications in quantum computing where electron spin would represent a bit of information (Lalena, and David, 2010, p. 359).

Conclusions

The magnetic field intensity and temperature effects on the magnetoresistivity of Tl_4Se_3S crystals have been studied. A negative magnetoresistivity has been observed. This character is explained by means of localized spin magnetic moment model in which carriers in an energy band are scattered by the localized spin of metallic atoms. The magnetoresistivity is observed to exhibit a semiconductor-metal transition associated with paramagnetic-ferromagnetic transition at a critical temperature of 270 K. This behavior is explained by considering the lattice and magnetic scattering exchange as well as the density of excited charge carriers.

References

1. Bellouz, R., Kallel, S., Khirouni, K., Pena, O., and Oumezzine M. (2015). Structural, Electrical Conductance and Complex Impedance Analysis of $(Nd_{1-x}Ce_x)_{0.7}Sr_{0.3}MnO_3$ ($0 \leq x \leq 0.20$) Perovskite. *Ceramics International*. 41(2). PP 1929–1936.
2. Bin, L., Qing, H., Mark, C., Yunhao, X., and Wei, T. (2015). "Tunneling Magneto-Resistive Sensors with Buffer Layers" United States Patent 20150097255.
3. Feng, M., Li, H., Liu, M., Li, N., and Zheng, W. (2009). Magnetic and Magnetoresistive Properties of $La_{0.65-x}Eu_xSr_{0.35}MnO_3$. *Ceramics International*. 35 (8). PP 345-347.

4. Guler, I. (2014). Low-Temperature Visible Photoluminescence and Optical Absorption in $\text{Tl}_2\text{In}_2\text{Se}_3\text{S}$ Semiconductor . *Journal of Applied Physics*. 115 (1-2). PP 033517.
5. Guseinov, G. D., Guseinov, S. G., Mustafaeva, S. N., Bagirzade, E. F., and Abdullaev E. G. (1986). P-TlSe Single Crystal — Based Accumulating Cell. *Materials Chemistry and Physics*. 14 (2). PP 181-185.
6. Isik, M., Yildirim, T., and Gasanly, N.M. (2015). Determination of Trapping Parameters of Thermoluminescent Glow Peaks of Semiconducting $\text{Tl}_2\text{Ga}_2\text{S}_3\text{Se}$ Crystals. *Journal of Physics and Chemistry of Solids*. 82(7). PP 56–59.
7. Kent, A. D., and Worledge, D. C. (2015). A New Spin on Magnetic Memories. *Nature Nanotechnology*. 10(3). PP 187–191.
8. Khosla, R. P., and Fischer, J. R. (1970). Magnetoresistance in Degenerate CdS: Localized Magnetic Moments. *Physical Review B*. 2(10) . PP 40-84.
9. Kokkinis, G., Jamalieh, M., Cardoso, F., Cardoso, S., Keplinger, F., and Giouroudi, I. (2015). Magnetic-Based Biomolecule Detection using Giant Magnetoresistance Sensors. *Journal of Applied Physics*. 117 (17). PP 17B731.
10. Lalena, J. N., and David, A. Cleary. (2010). *Principles of Inorganic Materials Design*, New Jersey .Wiley & Sons. PP 359.
11. Lekue, A. G., Balashov T., Olle, M., Ceballos, G., Arnau, A., Gambardella, P., Sanchez-Portal, D., and Mugarza, A. (2014). Spin-Dependent Electron Scattering at Graphene Edges on Ni(111). *Physical Review Letters*. 112(6). PP 066802.
12. May, S. J., Blattner, A. J., and Wessels, B. W. (2004). Negative Magnetoresistance in (In,Mn) as Semiconductors. *Physical Review B*. 70(7). PP 073303.
13. Ni, Y., Shao, M., Wu, Z., Gao, F., and Wei, X. (2004). The Effect of KI on the Formation of Tl_2E (E=S, Se) Nanorods Via Solvothermal Route. *Solid State Communications*. 130 (5). PP 297-300.
14. Nicolas, P., Melzer, M., Makarov, D., Ueberschar, O., Ecke, R., Schulz, S. E., and Schmidt, O. J. (2015). High-performance Giant Magnetoresistive Sensorics on Flexible Si Membranes. *Applied Physics Letters* 106(15). PP 153501.
15. Ohno, H., Munekata, H., Penney, T., Von, M. S., and Chang, L. L. (1992). Magnetotransport Properties of p-Type (In,Mn) as Diluted Magnetic III-V Semiconductors. *Physical Review Letters*. 68(17). PP 2664.

16. Pérez, N., Melzer, M., Makarov, D., Ueberschär, O., Ecke, R., Schulz, S. E. and Schmidt, O. G. (2015). High-Performance Giant Magnetoresistive Sensorics on Flexible Si Membranes. *Applied Physics Letters*. 106 (15). PP 153501.
17. Qasrawi, A. F., and Gasanly, N. M. (2006). Optical Properties of TlInS₂ Layered Single Crystals Near the Absorption Edge. *Journal of Materials Science*. 41(11). PP 3569-3572.
18. Qasrawi, A. F., and Gasanly, N. M. (2010). Properties of Tl₄Se₃S Single Crystals and Characterization of Ag/Tl₄Se₃S Schottky Barrier Diodes. *Current Applied Physics*. 10(2). PP 592-595.
19. Quan, Z., Zhang, Li, Liu, W., Zeng, H., and Xu, X. H. (2014). Resistivity Dependence of Magnetoresistance in Co/ZnO Films. *Nanoscale. Research Letters*. 9 (1). PP 6.
20. Shim, Y. Gu, Kawabata, T., Wakita, K., and Mamedov, N. (2015). Temperature Behavior of Dielectric Function Spectra and Optical Transitions in TlGaS₂. *Physica Status Solidi (b)*. 252(6). PP 1254-1257.
21. Yıldırım, T., Sülünhat, B., and Gasanly, N.M. (2015). Low Temperature Thermally Stimulated Current Measurements in N-Implanted TlGases Layered Single Crystals. *Materials Science in Semiconductor Processing*. 34 (6). PP 121–125.
22. Zalamai, V.V., Stamov, I.G., Syrbu, N.N. , Ursaki, V.V., and Dorogan, V. (2015). Resonance Raman Scattering and Excitonic Spectra in TlInS₂ Crystals. *Journal of Luminescence*. 160 (4). PP 195–201.

ظاهرة المقاومة المغناطيسية السالبة في بلورات Tl_4Se_3S

عاطف فايز قسراوي

قسم الفيزياء، كلية العلوم، الجامعة العربية الأمريكية-جنين

atef.qasrawi@aaup.edu

المخلص

تعالج هذه المقالة تأثير الحرارة وشدة المجال المغناطيسي على المقاومة المغناطيسية لبلورات Tl_4Se_3S في المدى الحراري من 195-310 ك والمدى المغناطيسي الذي تصل شدته إلى 1.4 تسلا. وقد لوحظ أن المقاومة المغناطيسية لهذه البلورات هي سالبة عند كل درجات الحرارة المقاسة، وفي حال تثبيت درجة الحرارة وزيادة شدة المجال المغناطيسي تزداد سالبية المقاومة المغناطيسية. ولتشخيص هذه الظاهرة النادرة المشاهدة في مثل هذا النوع من البلورات تم استخدام نموذج *Khosla-Fischer* الذي يركز على الانحراف الدوراني لحاملات الشحنة في مستويات الطاقة الناتجة من الشوائب في البلورة.

وقد بينت الدراسة الحرارية للمقاومة المغناطيسية أنه يوجد انتقال مرحلي من حالة البارامغناطيسية إلى الفرومغناطيسية عند درجة 270 ك وانتقال مرحلي من حالة الفرومغناطيسية إلى البارامغناطيسية عند 220 ك. ويعزى وجود هذه الانتقالات في النطاق الحراري من 220-270 ك إلى سيادة الانحرافات الدورانية المتمركزة وإلى هيمنة الانحرافات الحرارية الميكانيكية المصاحبة للأمواج الصوتية في النطاق المتبقي من الحرارة.

الكلمات المفتاحية: المقاومة، البلورات المتسلسلة، المغنطة، Tl_4Se_3S .